Analytica Chimica Acta 828 (2014) 27–33

Contents lists available at ScienceDirect

Analytica Chimica Acta

journal homepage: www.elsevier.com/locate/aca

A photoelectrochemical biosensor using ruthenium complex-reduced graphene oxide hybrid as the photocurrent signal reporter assembled on rhombic TiO_2 nanocrystals driven by visible light

Lei Ge [a], Yanhu Wang [a], Hongmei Yang [a], Ping Yang [b,c], Xin Cheng [b], Mei Yan [a], Jinghua Yu [a,*]

[a] School of Chemistry and Chemical Engineering, University of Jinan, Jinan 250022, PR China
[b] School of Material Science and Engineering, University of Jinan, 250022, Jinan, PR China
[c] State Key Laboratory of Crystal Materials, Shandong University, Jinan 250100, PR China

HIGHLIGHTS

- A sandwich-type photoelectrochemical immunosensor was fabricated.
- Highly crystalline rhombic TiO_2 NCs was prepared through solvothermal method.
- Ru complex was used as the photoelectrochemical signal-generating molecule.
- Ru complex hybridized RGO was prepared and used as signal amplification label.

GRAPHICAL ABSTRACT

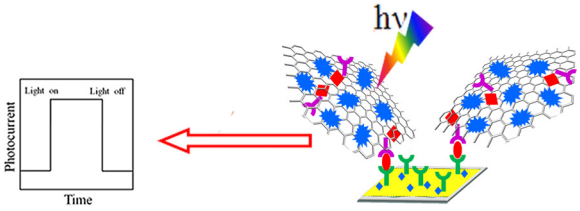

ARTICLE INFO

Article history:
Received 5 September 2013
Received in revised form 11 April 2014
Accepted 14 April 2014
Available online 21 April 2014

Keywords:
Immunoassays
Ru complex
Reduced graphene oxide
Rhombic TiO_2 nanocrystals
Photoelectrochemistry

ABSTRACT

An ultrasensitive photoelectrochemical (PEC) immunoassay of cancer biomarker carcinoembryonie antigen (CEA) is proposed that uses rhombic titanium dioxide nanocrystals (TiO_2 NCs) coupled with Ab2–RGO-Ru bioconjugate, which featured CEA signal antibody (Ab2) and ruthenium *tris*(bipyridine) (Ru complex) labels linked to reduced graphene oxide (RGO) for signal amplification. Herein, the Ru complex acts as an electron donor, while RGO serves as an electron acceptor which facilitates charge separation and suppresses recombination of photoexcited electron–hole pairs in the hybridized species. The rhombic TiO_2 NCs were fabricated through a solvothermal technique in anhydrous ethanol, followed by spin-coating process and calcination, an ITO/TiO_2 electrode was obtained. Chitosan (CS) and glutaraldehyde (GLD) were used to modify the prepared ITO/TiO_2 electrode to covalently immobilize antibodies. With a sandwich-type immunoreaction, CEA and Ab2–RGO-Ru were conjugated successively to form a sandwich-type immunocomplex. Thus, a sandwich-type PEC immunosensor was fabricated for the detection of CEA was developed by monitoring the changes in the photocurrent signals of the electrode resulting from the immunoreaction. The proposed PEC immunosensor showed high sensitivity, selectivity, excellent stability, and good reproducibility, and thus has great potential to be used for other biological assays.

1. Introduction

Tumor marker molecules occur in blood and tissues that are associated with cancer, and whose identification and

* Corresponding author at: Key Laboratory of Chemical Sensing and Analysis in Universities of Shandong (University of Jinan), School of Chemistry and Chemical Engineering, University of Jinan, Jinan 250022, China. Tel.: +86 531 82767161.
E-mail address: ujn.yujh@gmail.com (J. Yu).

http://dx.doi.org/10.1016/j.aca.2014.04.032
0003-2670/

determination are significant in cancer diagnosis and clinical therapy [1,2]. Hence, developing sensitive and accurate detection of disease-related biomarkers is critical to many areas of biomedical research and diagnosis [3], in particular, the clinical measurement of cancer biomarkers shows great promise for early diagnosis, disease monitoring, and highly reliable prediction [4]. As a tumor marker, carcinoembryonic antigen (CEA) known as one of the most important cancer biomarkers, was found on the surface of many ovarian cancer cells [5]. Thus, developing a rapid and sensitive detection method for CEA is of great importance in clinical research. Immunoassays, a promising approach for selective and sensitive analysis based on specific antigen–antibody interaction, have gained increasing attention in different fields [6–9]. There are several conventional immunoassays for CEA detection, such as enzyme-linked immunosorbent assay (ELISA) [10], electrochemistry [11], electrochemiluminescence (ECL) [12], mass spectrometry [13], quartz crystal microbalance (QCM) [14], and surface plasmon resonance (SPR) immunoassays [15]. However, there are some limitations of these methods for practical usages including the analysis complex, time consuming and expensive. Thus, there is an urgent need to develop operationally simple, highly sensitive, and inexpensive methods for the biomarkers detection.

Photoelectrochemical (PEC) analysis possesses the advantages of high selectivity and sensitivity due to the separation forms of excitation source and detection signal is a newly emerged yet dynamically developing technique for probing various biological events. During PEC detection, light is used to excite active species on the electrode, and photocurrent is obtained as the detection signal, which is just the reverse process of electrochemiluminescence (ECL). Coupling photoirradiation with electrochemical detection, the PEC sensors have the advantages of both optical and electrochemical sensors [16]. In addition, electronic detection instruments are simple, low-cost, and well-suited for rapid high-throughput biological assays. Thus, this technique shows promising analytical applications and has attracted considerable research interest.

Recent advances in semiconducting nanoparticles (NPs) or quantum dots (QDs) such as TiO_2, CdS, have shown great promise in PEC sensors due to their high fluorescence quantum yields, stability against photobleaching, and size-controlled luminescence properties [17–19]. As an important semiconductor nanomaterial, TiO_2-based composites have proved to be an excellent electrode material in PEC biosensing owing to their good biocompatibility, relative conductivity, low cost, environmental safety, and chemical and thermal stability [20]. However, the wide band gap of the bare TiO_2 could only be photoelectrochemically excited under UV irradiation which limits the utilization of solar light. Furthermore, the strong oxidation ability of photogenerated holes formed at illuminated TiO_2 may cause destructive effects for biomolecules [21]. Hence, many efforts have been made toward the development of TiO_2-based composites in visible-light activated PEC biosensing, which could largely increase the efficient utilization of solar light and reduce the destructive effect of UV light and the photo-generated holes of illuminated TiO_2 to biomolecules [22–25].

According to Guo's previous work [26–30], ruthenium derivative has been employed as the photoelectrochemical signal-generating molecule with porous SnO_2 film as semiconductor electrode due to their broad absorption and long excited-state lifetimes [31–33]. Herein, ruthenium *tris*(bipyridine) (Ru complex) was used as the photoelectrochemical signal-generating molecule integrated with the rhombic TiO_2 NCs modified ITO electrode in this work. Under the illumination of visible light, the Ru complex absorbs photon energy and becomes electronically excited. And the generated electrons injected into the conduction band of the TiO_2 electrode, produced Ru^{3+} species. Meanwhile, the ascorbic acid (AA) was employed as an efficient and nontoxic sacrificial electron donor to reduced Ru^{3+} back to Ru^{2+} and sustains the photocurrent.

In order to increase electron transfer efficiency and effectively inhibit the recombination of photoexcited charges in Ru complex. Graphene has drawn great attention owing to its outstanding electronic, optical, thermal and mechanical properties. Graphene has been used as a good candidate for the acceptor material in organic photovoltaic (OPV) applications due to its large donor/acceptor interfaces for charge generation and a continuous pathway for electron transfer [34]. The significantly improved photo-responses confirmed that graphene was a good candidate for the collection and transport of photogenerated charges. Herein, we prepared Ru complex functionalized reduced graphene oxide (RGO) nanocomposite (Ru-RGO) to label signal antibody (Ab2) for signal amplication. Owing to the photosensitizer molecules Ru complex contacting directly with the RGO sheet and the excellent electronic conductivity of RGO, combining Ru complex with RGO sheets could increase electron transfer efficiency and effectively inhibit the recombination of photoexcited charges. RGO here serves not only as a superior supporting matrix for anchoring the sensitizer molecules but also as an excellent electron mediator to adjust electron transfer.

In this work, a novel photoelectrochemical biosensing platform for CEA detection was developed using newly synthesized rhombic TiO_2 NCs electrode. Chitosan (CS) and glutaraldehyde (GLD) as biocompatible matrix with high permeability and good susceptibility to chemical modifications were coated on the surface of rhombic TiO_2 NCs electrode for further immobilization of CEA capture antibody (Ab1). Ru-RGO was labeled with Ab2 to form Ru-RGO–Ab2, which were used for signal amplication to enhance detection sensitivity. It was found that the RGO not only acts as a solid-state electron mediator, which facilitates charge separation, but also suppresses recombination of photoexcited electron–hole pairs in Ru. All these characteristics promote an excellent photoelectrochemical biosensor for CEA detection with high selectivity and sensitivity. Moreover, the established method could provide an approach for the design of photoelectrochemical immunosensors in the detection of other significant proteins.

2. Experimental

2.1. Chemicals and materials

Titanium(IV) isopropoxide (TIP), oleic acid (OA), oleylamine (OM), anhydrous ethanol, bovine serum albumin (BSA, 96–99%), chitosan (CS), glutaraldehyde (GLD), potassium ferricyanide, graphite powder, hydrazine solution (50 wt%) and ammonia solution (28 wt%) were purchased from Shanghai Chemical Reagent Co. (China). Carcinoembryonic antigen (CEA), the capture antibody (Ab1) and the signal antibody (Ab2) were gotten from Shanghai Linc-Bio Science Co. Ltd. (Shanghai, China). Ruthenium (II) *tris*(bipyridine)-NHS (Ru(bpy)$_3^{2+}$-NHS) ester was obtained from IGEN (Gaithersburg, MD).

All chemicals and solvents used were analytical grade or the highest purity available and were used as received. And all solutions were prepared using Milli-Q water (Millipore) as a solvent. Phosphate buffered solutions (PBS, pH 7.4) were prepared using 0.01 mol L^{-1} KH_2PO_4 and 0.01 mol L^{-1} Na_2HPO_4. The CEA was stored at 4 °C, and its standard solution was prepared daily with PBS solution as in use.

2.2. Apparatus

A 500 W Xe lamp equipped with a monochromator was used as the irradiation source (CHF-XM500 W, Beijing Changtuo, China). The excitation source was a 473 nm light emitting diode with an illumination area of 0.2 cm^2. Photocurrent was measured by the current–time curve experimental technique using a CHI 660D

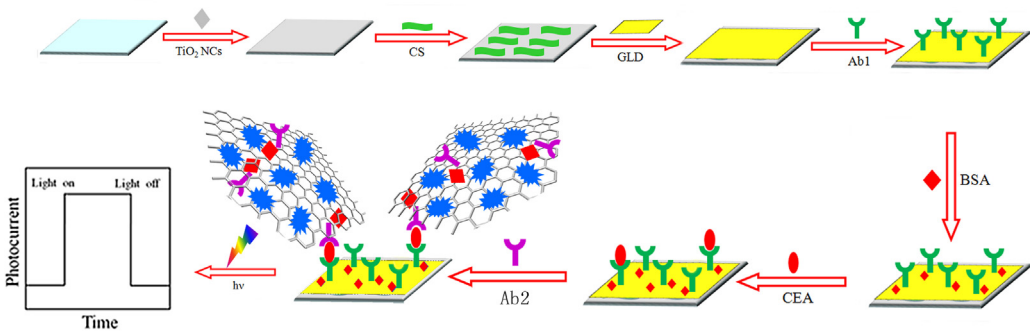

Scheme 1. Schematic representation of the fabrication of the proposed biosensor.

electrochemical workstation (Shanghai Chenhua, China) at a constant potential of 0 V with visible light irradiation. The scanning electron microscopy (SEM) images were recorded using a JEOL JSM-5510 scanning electron microscope. Transmission electron microscopy (TEM) images were obtained from a JEOL JEM-1400 microscope (Japan). The electrochemical impedance spectra (EIS) were obtained from a CHI 760D electrochemical workstation (Shanghai Chenhua). All experiments were carried out at room temperature using a conventional three-electrode system. Measurements were performed in 0.1 M pH 7.0 phosphate buffer solution (PBS) containing 0.1 M AA. During the PEC assay, PBS was purged with high-purity N_2 for 10 min and used as the electrolyte solution.

2.3. Synthesis of crystalline rhombic TiO_2 NCs

According to our previous work [35], the synthesis of crystalline rhombic TiO_2 NCs was synthesized through a facile solvothermal method. Typically, TIP of 5 mmol and OA of 20 mM were added into a 50 mL teflon cup and then shaked for 2 min. Then, the mixture of 30 mM of OM and 222 mM of anhydrous ethanol was added. After stirring for 10 min, the as-prepared mixture in a 50 mL teflon cup was put into a 100 mL teflon-lined stainless steel autoclave. The system was then heated at 180 °C for 22 h in an oven. The obtained white precipitates were washed several times with ethanol and then dried at room temperature. The morphology observation of rhombic TiO_2 NCs samples was performed using a transmission electron microscopy (TEM, JEOL JEM-1400).

2.4. Preparation of Ru complex functionalized RGO (Ru-RGO)

Functional groups could be introduced into graphene to form cations or cationic groups that could not only improve the solubility of graphene but also facilitate graphene assembly or reaction with other molecules, polymers and biological systems. Herein, primary amine was introduced into the RGO, and the amino modified (RGO–NH_2) was prepared according to previous study [36]. Then the Ru-RGO was obtained by adding 100 μg Ru $(bpy)_3^{2+}$-NHS ester predissolved in 1.5 mL DMSO to 0.5 mL of RGO–NH_2 PBS (pH 7.4) at room temperature. After 40 min incubation at room temperature in the dark, the mixture was filtered through a Sephadex G-25 PD-10 desalting column and eluted with PBS (pH 7.4). The purified Ru-RGO was further diluted with PBS (pH 7.4) to 1.0 mL and kept at 4 °C prior to use.

2.5. Preparation of Ru-RGO composite labeled Ab2

Firstly, 1.0 mL of obtained Ru-RGO was activated by 2.5% GLD (in 50 mM, pH 7.4 PBS) under ultrasound for 2 h and centrifuged to remove excess GLD. Then, 100 μL Ab2 (0.1 mg mL^{-1}) was added and the mixture was stirred gently at room temperature for 12 h, and centrifuged at 10,000 rpm for 10 min. After that the Ru-RGO composite labeled Ab2 were redispersed in 5 mL of 1% bovine serum albumin (BSA) solution containing 0.05% Tween for 2 h under stirring to block the excess amino group and nonspecific binding sites of the Ru-RGO composite labeled Ab2 nanospheres. After centrifuging and washing with PBS, finally the supernatant was removed and adjusted to a final volume of 5 mL with immobilization buffer, and stored at 4 °C prior to use.

2.6. Fabrication of photoelectrochemical immunosensor

The ITO slices were sonicated in acetone, NaOH (1 M) in ethanol/water mixture (1:1, v/v), and water, respectively, for 15 min each, followed by washing copiously with ultrapure water and dried at 120 °C for 2 h. The fabrication procedure of the immunosensor is shown in Scheme 1. A certain amount of obtained rhombus TiO_2 NCs powder was dispersed ultrasonically in water, and then 20 μL of the suspension was applied onto a piece of ITO slice with a fixed area of 0.2 cm^2. After drying in air, the film was sintered at 450 °C for 30 min in air atmosphere and finally naturally cooled down to room temperature. The thin film coated ITO is referred as ITO/TiO_2 NCs electrode. Twenty microliters of chitosan (CS) solution (0.05 wt%) prepared by dissolving chitosan powder in 1% acetic acid was dropped on ITO/TiO_2 NCs electrode and dried at room temperature. After the electrode was washed with 1.0 M NaOH and ultrapure water, respectively, 20 μL of 5% GLD solution was dropped onto the electrode and kept at room temperature for 30 min. Then the electrode was rinsed with ultrapure water thoroughly to remove physically adsorbed GLD. Afterwards, 20 μL Ab1 (50 μg mL^{-1}) was applied to the CS and GLD activated ITO/TiO_2 NCs electrode and allowing it to incubate for 30 min at room temperature. Then, it was rinsed with a washing buffer solution and incubated with 20 μL of blocking buffer solution (BSA) at room temperature for 30 min to block nonspecific binding sites. Subsequently, sample solutions (20 μL) containing different concentrations of CEA was added into the modified electrode and allowed to incubate for 30 min at room temperature followed by washing thoroughly with PBS. Finally, 20 μL the Ru-RGO–Ab2 composites were added to the corresponding location and allowed to incubate for 30 min at room temperature, followed by washing with washing buffer and ready to be used. The PEC experiments were performed in the quartz cell filled with 0.1 M pH 7.4 PBS at room temperature. For the PEC detections, under visible light irradiation, using a conventional three-electrode system with the modified ITO/TiO_2 electrode as the working electrode, a platinum wire as the auxiliary electrode and an Ag/AgCl electrode as the reference electrode, photocurrents were recorded in 0.1 M pH 7.0 PBS containing 0.1 M AA purged with high-purity N_2. The applied potential was 0 V. A 500 W Xe lamp equipped with monochromator used as a light source irradiated the prepared electrode. After

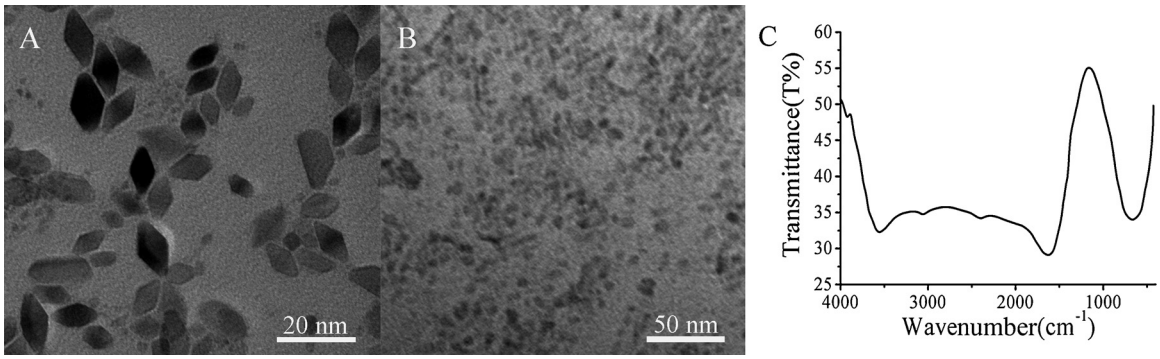

Fig. 1. The TEM images of prepared TiO_2 NCs at 180 °C (A) and 220 °C (B); (C) the FTIR spectrum of TiO_2 NCs prepared at 180 °C.

the background photocurrent was stabilized, the response was subsequently recorded as the excitation light turning on and off.

3. Results and discussion

3.1. Characterization of rhombic TiO_2 NCs

During the formation of rhombic TiO_2 NCs through a hydrolytic reaction, the morphology of resulting rhombus TiO_2 NCs samples depend strongly on the reaction temperature. The TEM morphologies of the prepared rhombic TiO_2 NCs using a TIP/OA/OM molar ratio of 1/2/3 at different temperature are clearly displayed in Fig 1A and B. As shown in Fig. 1A, sample prepared at 180 °C for 22 h, it is immediately apparent that the rhombic TiO_2 NCs are quite uniform, with an average size of 20 nm. The homogeneous film was beneficial for separation of the photon-generated carrier and then injected into the electrode. Compared with the sample prepared at 180 °C, TiO_2 NCs prepared at 220 °C (in Fig. 1B) revealed a broad size distribution and not regular morphologies.

Meanwhile, the FTIR spectrum of TiO_2 NCs prepared at 180 °C is presented in Fig. 1C. For bare rhombic TiO_2 NCs, there are three absorption bands, broad O—H stretching vibration peak centered at 3300 cm^{-1} associated with the vibration of —OH groups linked to surface Ti atoms and the stretching mode of adsorbed water molecules, a narrower band at 1620 cm^{-1} associated with the scissoring vibration of adsorbed water molecules and the absorbance between 500 and 730 cm^{-1} originated from the Ti—O—Ti bond of titanium dioxide [37].

3.2. Characterization of RGO, RGO–NH_2, and Ru-RGO

To verify the formation of the RGO–NH_2, the differences in FTIR spectrums (Fig. 2A) before and after amination were investigated. The FTIR of pristine RGO (in curve a) showed four obvious peaks at 1100, 1400, 1640 and 3445 cm^{-1} representing the stretching vibrations of C—O, C═C, carboxyl or conjugated carbonyl groups on the edge of the layer plane, and hydroxyl groups of RGO [38], respectively. Compared with RGO (in curve a), the RGO–NH_2 afforded bands at 1750, 1395, and 1100 cm^{-1}, which assigned to the C═O stretches of the —COOH groups, the —C—O—H deformation vibration peak, and the C—O—H stretch vibration, respectively [39,40]. And the peak at 1600 cm^{-1} becomes more sharp, and a new peak at 1210 cm^{-1} because of the torsional vibration, which attributed to the formation of amino on the surface of RGO.

SEM was also employed to characterize the RGO before and after the modification of Ru complex, respectively. Fig. 2B shows that the RGO is a single layer structure with smooth surface, no defect or hole can be observed on the surface. The well conjugated structure could facilitate the electron transfer, and was desirable to construct an electrochemical biosensing platform. After the formation of Ru-RGO, the surface of RGO became rough and the wrinkle could be seen (shown in Fig. 2C). And the result demonstrated that Ru-complex has been uniformly distributed on the surface of graphene, and the surface of graphene became much more rough. All these results confirmed that the Ru-complex had been successfully planted onto the surface of RGO with excellent dispersivity that prevented the agglomeration of Ru-complex.

3.3. EIS characterization of the immunosensor

Electrochemical impedance spectroscopy (EIS) measurement was utilized to monitor the fabrication process of the immunosensor. Fig. 3 shows the electrochemical impedance Nyquist plot of different modified electrodes using $[Fe(CN)_6]^{3-/4-}$ as redox probe. Curve a that shows a semicircle with a small diameter of the bare ITO electrode, indicats that the redox process of the $[Fe(CN)_6]^{3-/4-}$ probe shows a low electron-transfer resistance. While, after the formation of ITO/TiO_2 electrode, a much higher resistance was observed (curve b), and the phenomenon was ascribed to the rhombic TiO_2 NCs which could block the electron

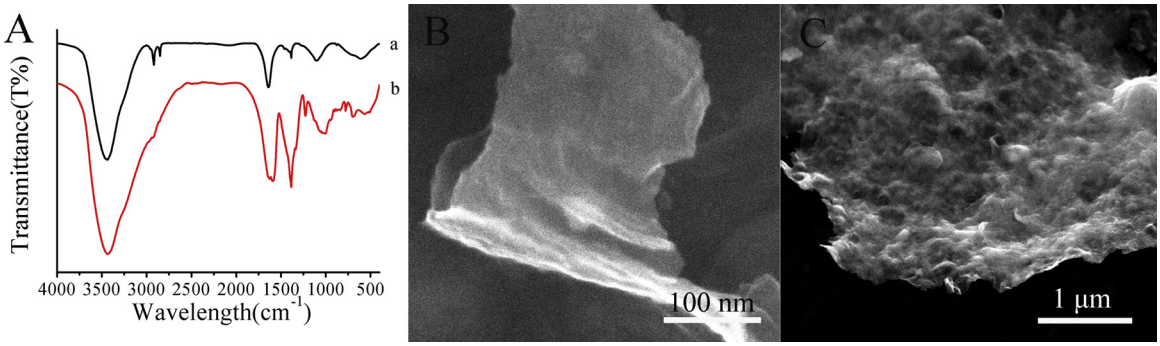

Fig. 2. (A) The FTIR spectra of RGO (a) and RGO–NH_2 (b); the SEM images of bare RGO (B) and Ru-RGO (C).

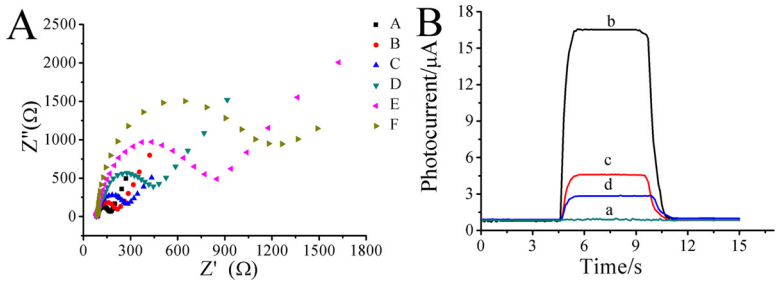

Fig. 3. (A) EIS of bare ITO (a), modified with TiO_2 NCs (b), modified with Ab1 (c), blocked by BSA (d), hybridization with CEA (e) and hybridization with the Ru-RGO labeled Ab2 (f). (B) The variation of the photocurrent of the proposed immunesensor during the fabrication process, bare ITO electrode (a), rhombus TiO_2 NCs modified ITO electrode (b), after the immobilization of 1 ng mL^{-1} CEA (c) and 10 pg mL^{-1} CEA (d) under visible light.

transfer. The result demonstrated that the rhombic TiO_2 NCs had been successfully deposited on the ITO electrode. When Ab1 was introduced into the ITO/TiO_2 NCs electrode, the diameter of the high frequency semicircle increased again (Fig. 3A, curve c), which might be ascribed to the fact that the Ab1 could hinder the electron transfer between the electrode and electrolyte, and the result suggested that the successful immobilization of Ab1 formed an additional barrier and further prevented the redox probe to the ITO electrode surface. After the modified electrode was blocked with BSA (Fig. 3A, curve d), the diameter of the high frequency semicircle increased further. The reason for the resistance increase was that the non-conductive properties of proteins would act as an inert layer, obstructing the diffusion of the redox probe to the electrode. The result also showed that BSA was successfully immobilized on the electrode surface. After that, the as obtained electrode was incubated with the CEA (Fig. 3A, curve e), the resistance further increased due to the formation of the immunocomplex. In the final step, the attachment of Ru-RGO–Ab2 bioconjugates gave rise to an additional barrier towards the access of the redox probe to the electrode, which resulted in a further increase in the electrode-transfer resistance (Fig. 3A, curve f).

3.4. Photoelectrochemical sensing response and mechanism

In the proposed PEC immunosensor, Ru complex, the photo-electrochemical signal reporter, upon illumination, absorbs photon energy and becomes Ru^{3+} and produces electron. Injection of the excited electrons into the conduction band of TiO_2 NCs through RGO produces photocurrent. The AA in the electrolyte was used as an electron donor to regenerate Ru^{2+}. Without the addition of the CEA, the Ru-RGO–Ab2 could not be immobilized on the prepared electrode, resulting in low photo-current response. However, in the presence of CEA, the Ru-RGO–Ab2 could be bound onto the prepared electrode through immunoreaction between antigen and antibody. The increasing amount of Ru-RGO–Ab2 bound to the prepared electrode resulted in a higher yield of photocurrent. As a result the generated photocurrent was proportional to the CEA concentration. Fig. 3B shows the photocurrent generated of the proposed immunesensor under visible light irradiation. The photocurrent of the proposed immunosensor appeared immediately upon irradiation and fell down instantly when the irradiation was cut off. First, there was no significant photocurrent detected on the bare ITO electrode (curve a). After the formation of rhombic TiO_2 NCs film on ITO, a large photocurrent was observed (curve b). Then the photocurrent decreased sharply after the modification of the electrode because of the prevention of AA from scavenging photogenerated holes on the film [41]. With the increase of CEA concentration more Ru-RGO–Ab2 were immobilized on the modified electrode leading to the increase of photocurrent (curve c and d).

3.5. Optimization of experimental conditions

The proposed immunesensor was designed for widely use, hence, the incubation temperature and time are important for its low-cost and portable applications. To obtain high sensitivity, the effect of temperature, incubation time and the pH value on the photocurrent intensity were investigated in this work. Here we choose room temperature as the reaction incubation temperature. The incubation time, a bottleneck to the improvement of assay speed in an immunoassay, would affect the time efficiency of the method. The effect of incubation times for PEC immunoassay was examined at room temperature (Fig. 4A). With an increasing incubation time, the photocurrent intensities increased quickly and reached their maximum values at 30 min. Therefore, subsequent experiments employed 30 min as the optimum time for all the incubation steps of the assay. As the pH of the detection solution might influence not only the PEC performance of the immunoassay, but also the activity of immobilized immune-proteins, the study of pH influence on the photocurrent intensity was conducted in the range of 6.0–8.0 in the detection solution containing 0.1 M AA. As shown in Fig. 4B, the immunosensor

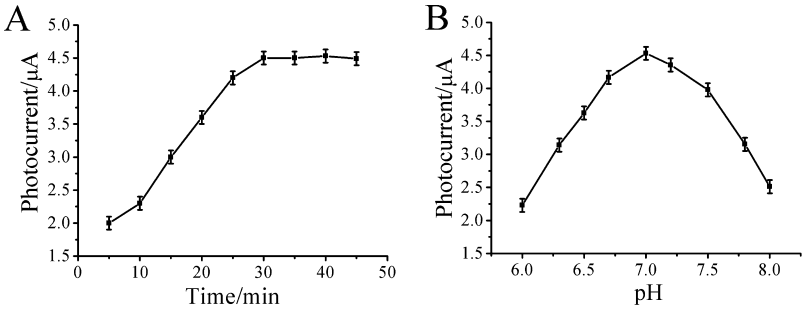

Fig. 4. Parameters affecting PEC signals, effects of incubation time (A) and pH (B).

Table 1
Comparison of analytical properties of different immunoassays toward CEA.

Immunoassay format	Linear range ($ng\,mL^{-1}$)	Detection limit ($pg\,mL^{-1}$)	Refs.
Electrochemical	0.5–120	400	[42]
Electrochemiluminescence	1.0–100	500	[43]
Electrochemical	0.0025–2	1.4	[44]
Electrochemical	0.01–160	5	[45]
Photoelectrochemistry	0.0001–100	0.059	This work

showed an optimal photocurrent response at pH 7.0. Thus, the optimal pH of 7.0 was chosen in the further study.

3.6. Photoelectrochemical response of the immunosensor to CEA

Under the optimal conditions, to assess the sensitivity and the quantitative range of the proposed immunoassay, the analytical performance of the proposed PEC immunesensor was explored by quantifying the different concentrations of the CEA solution, and the calibration graph for the determination of CEA is shown in Fig. 5A and B. Fig. 5A and B illustrates the photocurrent response of the proposed PEC immunesensor toward the CEA at different concentrations, indicating that the photocurrent response is proportional to the CEA concentrations, and exhibited a good linear relationship with the logarithm of CEA concentration from $0.1\,pg\,mL^{-1}$ to $100\,ng\,mL^{-1}$. The regression equation was $I = 2.04 + 0.754\,lg\,(c_{CEA}, pg\,mL^{-1})$ with the correlation coefficient of 0.992. And the relative standard deviation of this method was below 3.6% in 11 repeated measurements. The detection limit corresponding to three times the standard deviation of the blank solution was estimated to be $0.059\,pg\,mL^{-1}$. When compared with other sensors reported previously (Table 1), the proposed immunosensor exhibited a satisfactory detection limit and wide linear range. In this work, a sandwich-type PEC immunosensor for measurement of biomarkers was constructed, during the photoelectrochemical detection, light is used to excite active species on the electrode. Due to its separate source for excitation and detection, high sensitivity and low detection limit can be obtained. RGO, which has large surface-to-volume ratios, shows good promise to improve the performance of a photovoltaic device. The rhombic TiO_2 NCs with high photocatalytic activity, was used to modify ITO electrode. Meanwhile, Ru-RGO nanocomposite as an excellent label with signal amplification played an important role in improving the linear range and low detection limit.

3.7. Selectivity, reproducibility and stability of the immunosensor

To verify the specificity of the proposed PEC immunosensor for CEA detection, experiments were performed by using some structurally related interference in human serum, such as α-fetoprotein (AFP), cancer antigen 125 (CA125), human serum albumin (HSA) and prostate-specific antigen (PSA). The PEC immunosensor was incubated with $1.0\,ng\,mL^{-1}$ CEA containing different antigens ($1.0\,ng\,mL^{-1}$ AFP, $10.0\,U\,mL^{-1}$ CA 125, $1.0\,ng\,mL^{-1}$ HAS 153, and $1.0\,ng\,mL^{-1}$ PSA). The photocurrent responses to each type of antigen (100 nM) were recorded in Fig. 5C. The interference degree of variability between different tumor markers was acceptable.

Reproducibility was a very important feature for an immunosensor, it was necessary to investigate this feature of the developed immunosensor. The reproducibility of the proposed PEC immunosensor was evaluated by intra- and interassay coefficient of variations (CVs). The intra-assay CV was the difference between 11 determinations of one sample on the same ITO electrode with regeneration procedure [46] between each determination. The interassay CV was the difference between the measurements of the same sample on eleven different ITO electrodes. And the relative standard deviation (RSD) of the intraassay between six runs was 2.4% for $1.0\,ng\,mL^{-1}$ CEA; whereas, the RSD of the interassay with various batches was 4.3% for CEA, respectively. The result indicated that the proposed immunosensor possessed good precision and reproducibility, and further verified the possibility of batch preparation.

The stability of array immunosensor was also examined. When the immunosenor and Ru-RGO–Ab2 were not in use, they could be stored in the refrigerator at 4 °C, and they were measured at intervals of one week. It retained 93.9% of its initial response after a storage period of 2 months. These results indicated that this prepared immunosensor with good reproducibility, precision, and stability, during manufacture, storage or long-distance transport to remote regions and developing countries.

3.8. Application in analysis of serum samples

To evaluate a potential application of the immunoarray system, serum samples obtained from Shandong Cancer Hospital were assayed using the proposed method in this work as well as the reference values obtained by commercially used full-automatic electrochemiluminescence immunology analyzer (Roche Cobas E601) in Cancer Research Center of Shandong Tumor Hospital. When the levels of tumor markers were over the calibration ranges, serum samples were appropriately diluted with 10.0 mM pH 7.4 PBS prior to assay. Different amounts of CEA were added into human serum sample for recovery tests. The results are listed in Table 2, which shows acceptable results with relative errors less than 4.1% for CEA detection and recoveries between 98.7% and 102.0% for the CEA recovery experiment, which indicates good accuracy and precision of the proposed method.`

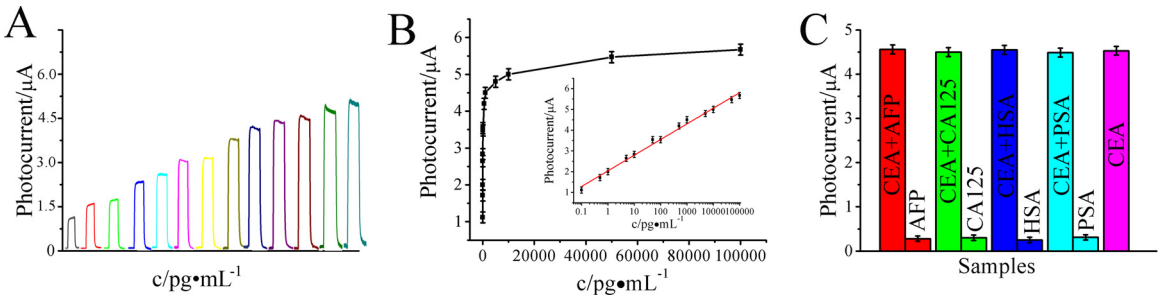

Fig. 5. (A) PEC signals of the immunosensor incubated with different concentrations ($pg\,mL^{-1}$) of CEA (from $0.1\,pg\,mL^{-1}$ to $100\,ng\,mL^{-1}$); (B) relationship between photocurrent ntensity and CEA concentration, each point was the average of five measurements. Inset: logarithmic calibration curve for CEA. (C) Selectivity of the PEC immunosensor.

Table 2
Comparison of CEA determinations using the proposed and reference methods.

Samples	Proposed method ($pg\,mL^{-1}$)	Reference method ($pg\,mL^{-1}$)	Relative error (%)	Added	Found	Recovery (%)
1	25.32	26.02	−2.76	1.0	0.98	98.0
2	34.78	33.36	4.02	10.0	10.13	101.3
3	42.59	44.31	−4.04	50.0	49.89	99.78
4	108.52	105.41	2.87	100.0	98.76	98.76
5	157.68	161.47	−2.40	150.0	148.35	98.9

[a]Average of 11 measurements.

4. Conclusions

In summary, an ultrasensitive photoelectrochemical immunosensor of cancer biomarker carcinoembryonic antigen (CEA) was developed on rhombic TiO_2 NCs modified ITO electrode. The ITO/TiO_2 electrode played an essential role in not only the immobilization of the protein molecules, but also the photocurrent generation during the assay process. The secondary antibody and Ru complex were bound to the reduced graphene oxidation (RGO) to yield Ru-RGO–Ab2 bioconjugates. Through an immunoreaction of antibody and antigen, an immunosensor with a sandwich structure was formed. Upon visible irradiation, the greatly enhanced sensitivity was obtained first by the fast electron migration from excited Ru complex to rhombic TiO_2 NCs. The sensitivity was further improved by the electron conductivity of the RGO which could also facilitate charge separation and suppress recombination of photoexcited electron–hole pairs in Ru complex. Results indicated that the photoelectrochemical immunosensor for CEA detection had good performance with high sensitivity, acceptable fabrication reproducibility, and excellent stability. Moreover, the designed immunosensor opened up a new perspective for the application of photoelectrochemistry, and might be of great importance for clinical and biological analysis of a wide range of significant proteins.

Acknowledgements

This work was financially supported by Natural Science Research Foundation of China (21277058, 21175058, 51003039) and Natural Science Foundation of Shandong Province, China (ZR2012BZ002).

References

[1] S.S. Gambhir, Nature Reviews Cancer 2 (2002) 683–693.
[2] M.S. Wilson, W.Y. Nie, Analytical Chemistry 78 (2006) 6476–6483.
[3] H. Kitano, Science 295 (2002) 1662–1664.
[4] P.R. Srinivas, B.S. Kramer, S. Srivastava, Lancet Oncology 2 (2001) 698–704.
[5] M. Zhang, S.G. Ge, W.P. Li, M. Yan, X.R. Song, J.H. Yu, W. Xu, J.D. Huang, Analyst 137 (2012) 680–685.
[6] C.X. Lei, F.C. Gong, G.L. Shen, R.Q. Yu, Sensors and Actuators B 96 (2003) 582–588.
[7] Y. Takahashi, A. Shevchuk, P. Novak, Y. Murakami, H. Shiku, Y. Korchev, T. Matsue, Journal of the American Chemical Society 132 (2010) 10118–10126.
[8] H.J. Lee, S.H. Lee, T. Yasukawa, J. Ramón-Azáon, F. Mizutani, K. Ino, H.T. Shiku Matsue, Talanta 81 (2010) 657–663.
[9] A. Dey, A. Kaushik, S.K. Arya, S. Bhansali, Journal of Materials Chemistry. 22 (2012) 14763–14772.
[10] J.A. Brochot, I.W. Siddiqi, Analytica Chimica Acta 224 (1989) 329–337.
[11] X.P. Liu, H.W. Wu, Y. Zheng, Z.S. Wu, J.H. Jiang, G.L. Shen, R.Q. Yu, Electroanalysis 22 (2010) 244–250.
[12] Y.L. Cao, R. Yuan, Y.Q. Chai, L. Mao, X. Yang, S.R. Yuan, Y.L. Yuan, Y.H. Liao, Electroanalysis 23 (2011) 1418–1426.
[13] S.H. Hu, S.C. Zhang, Z.C. Hu, Z. Xing, X.R. Zhang, Analytical Chemistry 79 (2007) 923–929.
[14] S.F. Chou, W.L. Hsu, J.M. Hwang, C.Y. Chen, Clinical Chemistry 48 (2002) 913–918.
[15] Y. Teramura, H. Iwata, Analytical Biochemistry 365 (2007) 201–207.
[16] X.R. Zhang, Y.S. Guo, M.S. Liu, S.S. Zhang, RSC Advances 3 (2013) 2846–2857.
[17] H.J. Zhao, D.L. Jiang, S.Q. Zhang, K. Catterall, R. John, Analytical Chemistry 76 (2004) 155–160.
[18] W. Lu, G. Wang, Y. Jin, X. Yao, J.Q. Hu, J.H. Li, Applied Physics Letters 89 (2006) 263902.
[19] H.B. Yildiz, R. Freeman, R. Gill, I. Willner, Analytical Chemistry 80 (2008) 2811–2816.
[20] J.X. Qiu, S.Q. Zhang, H.J. Zhao, Sensors and Actuators B 160 (2011) 875–890.
[21] G.L. Wang, J.J. Xu, H.Y. Chen, S.Z. Fu, Biosensors and Bioelectronics 25 (2009) 791–796.
[22] H. Tokudome, Y. Yamada, S. Sonezaki, H. Ishikawa, M. Bekki, K. Kanehira, M. Miyauchi, Applied Physics Letters 87 (2005) 213901.
[23] D. Chen, H. Zhang, X. Li, J.H. Li, Analytical Chemistry 82 (2010) 2253–2261.
[24] H.B. Li, J. Li, Q. Xu, X.Y. Hu, Analytical Chemistry 83 (2011) 9681–9686.
[25] Q. Kang, L.X. Yang, Y.F. Chen, S.L. Luo, L.F. Wen, Q.Y. Cai, S.Z. Yao, Analytical Chemistry 82 (2010) 9749–9754.
[26] B.T. Zhang, L.H. Guo, M.M. Greenberg, Analytical Chemistry 84 (2012) 6048–6053.
[27] M.M. Liang, S.L. Liu, M.Y. Wei, L.H. Guo, Analytical Chemistry 78 (2006) 621–623.
[28] D. Dong, D. Zheng, F.Q. Wang, X.Q. Yang, N. Wang, Y.G. Li, L.H. Guo, J. Cheng, Analytical Chemistry 76 (2004) 499–501.
[29] Y.P. Wu, B.T. Zhang, L.H. Guo, Analytical Chemistry 85 (2013) 6908–6914.
[30] B.T. Zhang, L.H. Guo, Biosensors and Bioelectronics 37 (2012) 112–115.
[31] A. Juris, V. Balzani, F. Barigelletti, S. Campagna, P. Belser, A. von Zelewsky, Coordination Chemistry Reviews 84 (1988) 85–277.
[32] K. Kalyanasundaram, Coordination Chemistry Reviews 46 (1982) 159–244.
[33] L. Sun, L. Hammarstrom, B. Akermark, S. Styring, Chemical Society Reviews 30 (2001) 36–49.
[34] X. Wan, G. Long, L. Huang, Y. Chen, Advanced Materials 23 (2011) 5342–5358.
[35] L. Ge, P. Yang, X. Cheng, Journal of Nanoscience and Nanotechnology (2014), doi:10.1166/jnn.2013.8623.
[36] M. Yan, D.J. Zang, S.G. Ge, L. Ge, J.H. Yu, Biosensors and Bioelectronics 38 (2012) 355–361.
[37] Y.X. Zhang, G.H. Li, Y.C. Wu, Y.Y. Luo, L.D. Zhang, Journal of Physical Chemistry B 109 (2005) 5478–5481.
[38] C. Nethravathia, T. Nishaa, N. Ravishankarb, C. Shivakumarac, M. Rajamathia, Carbon 47 (2009) 2054–2059.
[39] H.L. Guo, X.F. Wang, Q.Y. Qian, F.B. Wang, X.H. Xia, ACS Nanotechnology 3 (2009) 2653–2659.
[40] Y.C. Si, E.T. Samulsk, Nano Letters 8 (2008) 1679–1682.
[41] G.L. Wang, P.P. Yu, J.J. Xu, H.Y. Chen, Journal of Physical Chemistry C 113 (2009) 11142–11148.
[42] F. Tan, F. Yan, H.X. Ju, Electrochemistry Communications 8 (2006) 1835–1839.
[43] L. Ge, J.X. Yan, X.R. Song, M. Yan, S.G. Ge, J.H. Yu, Biomaterials 33 (2012) 1024–1031.
[44] G.S. Lai, F. Yan, H.X. Ju, Analytical Chemistry 81 (2009) 9730–9736.
[45] D.P. Tang, R. Yuan, Y.Q. Chai, Analytical Chemistry 80 (2008) 1582–1588.
[46] Z.J. Yang, Z.Y. Xie, H. Liu, F. Yan, H.X. Ju, Advanced Functional Materials 18 (2008) 3991–3998.